GPS radio occultation technique for measurement of the atmosphere above tropical cyclones

Biondi, Riccardo; Neubert, Torsten; Syndergaard, Stig; Nielsen, Johannes

Published in:
2nd International COSPAR Colloquium -

Publication date:
2009

Document Version
Publisher's PDF, also known as Version of record

Citation (APA):
Biondi, R., Neubert, T., Syndergaard, S., & Nielsen, J. (2009). GPS radio occultation technique for measurement of the atmosphere above tropical cyclones. In *2nd International COSPAR Colloquium -: Scientific and Fundamental Aspects of the Galileo Programme* (Vol. wpp 302 Proceeding)

GPS RADIO OCCULTATION TECHNIQUE FOR MEASUREMENT OF THE ATMOSPHERE ABOVE TROPICAL CYCLONES

Riccardo Biondi (1), Torsten Neubert (1), Stig Syndergaard (2), Johannes Nielsen (2)

(1) *DTU Space, National Space Institute, Juliane Maries Vej 30, 2100, København Ø, Denmark*
ribi@space.dtu.dk, neubert@space.dtu.dk
(2) *DMI, Danish Meteorological Institute, Lyngbyvej 100, 2100, København Ø, Denmark*
ssy@dmi.dk, jkn@dmi.dk

ABSTRACT

Water vapour transport to the upper troposphere (UT) and lower stratosphere (LS) by deep convective storms affects the radiation balance of the atmosphere and has been proposed as an important component of climate change [1-4]. The aim of the work presented here is to understand if the GPS Radio Occultation (RO) technique applied to a GPS receiver on the International Space Station (ISS) [5] will be useful for characterisation of this process. Our initial assessment presented here, addresses the question if severe storms leave a significant signature in RO profiles in the upper troposphere/lower stratosphere (UT/LS). The result is positive, suggesting that the bending angle of a GPS signal contains interesting information on the atmosphere around the tropopause. The presentation is focused on one particular Tropical Cyclone (TC), the hurricane Bertha, which formed in the Atlantic Basin during July 2008 and reached a maximum intensity of Category 3.

1. INTRODUCTION

The International Space Station (ISS) is an interesting platform for observations of deep convective storms because the orbit inclination of 51.6° allows instruments to monitor the major convective storm regions of the earth. An advanced GPS receiver is planned for the ISS as part of the ACES [5] payload and a number of optical cameras for the ASIM payload [6]. Both payloads will be mounted on the external platforms of the ESA Columbus laboratory module and be viewing primarily towards the limb in the forward direction. With these instruments the ISS may potentially secure a unique data set on tropopause water vapour transport and content. The water vapour content in the Earth's upper troposphere/lower stratosphere (UT/LS) is an important climate parameter. Like CO_2, stratospheric water vapour acts like a greenhouse gas, contributing to global warming of the atmosphere. Despite its relative diluteness, changes in stratospheric water vapour mixing ratio since 1960 could have accounted for up to 40% of the radiative forcing due to well-mixed greenhouse gases [7]. In the last 25 years, several instruments have become available to study atmospheric water vapour, and many studies show the increase of water vapour in the UT during this period [8]. It is also well known that deep convection from storms increases the relative humidity in the tropics [4] [9-11]. In this way, Tropical Cyclones (TCs) should play an important role since they lead to deep convective activity. Although they are not frequent, they are larger than other tropical convective systems, exist for longer time and persist in the same areas for many hours or days with vigorous convective towers. The overshooting clouds in the tropics are usually outside of TCs, but there are some areas where overshoots are mostly due to TCs. In general they account for only 7% of the deep convection in the tropics but they contribute 15% of the convection that overshoot the tropopause [12]. Such TCs increase the water vapour content of the UT [13] and the integrated water vapour in the vicinity of the storm [14]. Moreover, they warm the mid troposphere and they cool the tropopause layers [15-17].

The GPS radio occultation (RO) technique [18] is useful for studying severe weather phenomena because the GPS signals penetrate through clouds and allow measurements of atmospheric profiles related to temperature, pressure, and water vapour with high vertical resolution. We have analyzed GPS RO profiles during severe storms to understand if they provide significant information on the convection in the UT/LS. The storm systems studied are TCs which are known to reach high altitudes and may have a relatively large horizontal extent. GPS data from RO experiments onboard GPS/MET [19], CHAMP [20], SAC-C [21], and the COSMIC six-satellite constellation [22] were analyzed in relation to TC positions for the period 1996-2008, identifying several hundred ROs that coincide with TC positions. Whereas no evident variation at the tropopause is seen in the high-level RO data products such as water vapour, pressure and temperature profiles, the GPS signal refractive index profile and especially the bending angle profile, show a TC signature in the upper troposphere.

The work presented here is focused on one particular TC, the hurricane Bertha, which formed in the Atlantic Basin during July 2008 and reached a maximum intensity of Category 3. Using measurements from a variety of earth observation satellites and from aircraft, together with the best track information provided by the US National Hurricane Center (NHC), we reconstructed the characteristics of Bertha and compared them to ROs from the COSMIC mission. The RO profiles were selected in a time window dependent on the TC advection velocity and a space window dependent on the TC radius and eye radius. The profiles of the selected ROs were then compared to those of an undisturbed atmosphere in the same region and during the same month.

2. DATA DESCRIPTION

2.1. Tropical Cyclones Best Track

The tropical cyclones best tracks were collected from different sources: US National Hurricane Center (Atlantic, Carribean, Gulf of Mexico and Eastern Pacific), Australian Government Bureau of Meteorology (Western, Northen, Eastern Australia), Japan Meteorological Agency (Western, Northern Pacific), Meteo France (SouthWest Indian Basin) and Unysis Weather (North Indian Ocean Basin, Bay of Bengal and Arabian Sea). These sources usually provide information every 6 hours, including at least the name, coordinates, dates, pressure, maximum wind speed and category of the tropical cyclone. In some cases additional information is available, such as eye dimension (from Hurricane Hunters missions), moving cyclone direction, and speed.

2.2. GPS Radio Occultations

The GPS/MET, CHAMP, SAC-C, and COSMIC GPS Radio Occultations that we have analysed were downloaded from the COSMIC Data Analysis and Archive Center (CDAAC). For the analysis of TCs we first selected the ROs within 400 km from the TC eye and within a time window of 3 hours. In this paper we present results from the COSMIC level2 products:

- atmPrf: containing so-called dry pressure and temperature (derived assuming no water vapour [19]), refractivity, bending angle, and impact parameter versus geometric height above mean sea level
- wetPrf: containing pressure, temperature and moisture (derived via a 1-dimensional variational approach using ECMWF low resolution analysis data) interpolated to 100 meter height levels
- ecmPrf: containing pressure, temperature and moisture profiles generated from the ECMWF gridded analysis and co-located with occultation profiles.

2.3. A-TRAIN instruments

All the instruments that we used for comparisons are onboard the A-Train satellites, a satellite formation, consisting of six satellites flying in close proximity in a sun-synchronous polar orbit. We used data from the following four instruments in the A-Train:

The Atmospheric Infrared Sounder (AIRS) on the AQUA satellite provides profiles of temperature and pressure within 28 layers and water vapour content within 14 pressure layers up to 50 hPa. The horizontal resolution is 45 km and the vertical resolution roughly 2 km in the troposphere. We used level 2 data version 5.0, selecting the “Pgood” measurements and rejecting the layers for which the water vapour content is lower than the sensitivity.

The Moderate Resolution Imaging Spectroradiometer (MODIS) on the AQUA satellite provides high radiometric sensitivity in 36 spectral bands in the visible and near infrared channels, ranging in wavelength from 0.4 µm to 14.4 µm. We used MOD05 products to monitor the tropical cyclone diameter.

The Cloud-Aerosol Lidar with Orthogonal Polarization (CALIOP) on the CALIPSO satellite provides high-resolution vertical profiles of aerosols and clouds. For our purposes we used lidar level 1 products version 2.01 providing 33 pressure, temperature and relative humidity levels with a vertical resolution close to 2 km. We used these products as comparisons for temperature and relative humidity profiles.

The Microwave Limb Sounder (MLS) on the Aura satellite provides measurements of temperature and mixing ratio with a vertical resolution in the upper troposphere around 3 km. The resolution is very low in the upper troposphere but it is good enough to get a trend of those two parameters. We used for this work level 2 products version 2.2.

3. CASE STUDY: HURRICANE BERTHA

Hurricane Bertha formed at the beginning of July 2008 near the West African coast and it became an extra tropical cyclone on 20th of July. During its life, Bertha moved westward and increased in strength from tropical storm to hurricane category 3 in 4 days, maintaining hurricane status for several days. The track of Bertha is shown in Fig.1.

For different reasons Bertha was our best choice. First of all, Bertha´s track was long in time and space, increasing the probability to find ROs suitable for our studies. Eight COSMIC occultations were found close enough to hurricane Bertha in space and time. Moreover the long period in TC condition, allowed us to distinguish possible differences with tropical storm condition. Last but not least, in the same area there was not any other TC for a long time (the previous one was in 2007 and the next one two months later) so the upper tropospheric variations in that area were probably only due to hurricane Bertha.

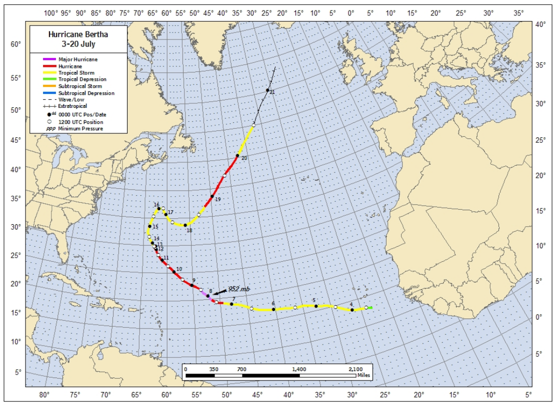

Figure 1. Bertha´s track from US NHC. Yellow line is tropical storm, red line is hurricane and purple line is major hurricane

We used US NHC best track database as reference, providing date, time, coordinates, pressure and wind speed every 6 hours. We added information on the cyclone diameter using MODIS data, on the cyclone eye dimension using Hurricane Hunters dataset, and finally we computed the moving speed.

Only the ROs within the radius of the TC and the radius of the eye (when available) in a time window of 3 hours, were analysed. Tab. 1 shows the times of the RO events and the other datasets available for this study.

TC	COSMIC	CALIPSO	MLS
08/07 00.00	08/07 02.01		
08/07 12.00	08/07 14.19	08/07 16.50	08/07 13.30
10/07 06.00	10/07 05.34	10/07 05.58	10/07 02.00
10/07 06.00	10/07 04.36	10/07 05.58	10/07 02.00
11/07 18.00		11/07 17.21	11/07 13.30
12/07 12.00	12/07 12.37		
12/07 12.00	12/07 12.47		
13/07 12.00		13/07 17.09	13/07 13.30
18/07 00.00	18/07 02.44		
19/07 00.00	19/07 02.07		

Table 1. Correspondences between Bertha´s track and other satellite measurements

4. PROFILES ANALYSIS

The GPS receiver on COSMIC measures the phase and amplitude of two L-band signals. The bending angle is calculated from the phase and amplitude and refractivity is computed using Abel inversion. Details of the RO processing at CDAAC can be found in [23]. Temperature, pressure and water vapour is derived via a 1-dimensional variational (1Dvar) approach involving the refractivity and the ECMWF model. The particular implementation of the 1Dvar at CDAAC weights the refractivity observation much more than the model, giving a solution in which the temperature (*T* in Kelvin), pressure (*p* in mb), and water vapour pressure (*e* in mb) are basically consistent with the derived refractivity, *N*, according to

$$N = 77.6\frac{p}{T} + 3.73 \cdot 10^5 \frac{e}{T^2} \qquad (1)$$

We first analyzed temperature, pressure, and water vapour profiles above the TC, focusing the attention on the upper troposphere, but we did not find any evident signature. Analysis of bending angle profiles however, provided interesting information.

Shown in Fig. 2 is an example of bending angle signature during Hurricane Bertha. The parameter plotted here is the bending angle percentage anomaly with respect to the annual mean value $(\alpha_{TC} - \alpha_{Annual})/\alpha_{Annual}$, where α_{TC} is bending angle value during the tropical cyclone and α_{Annual} is the annual average bending angle exactly in the same area covered by the cyclone. To get the annual average we collected all the ROs of 2008 within the diameter of Bertha.

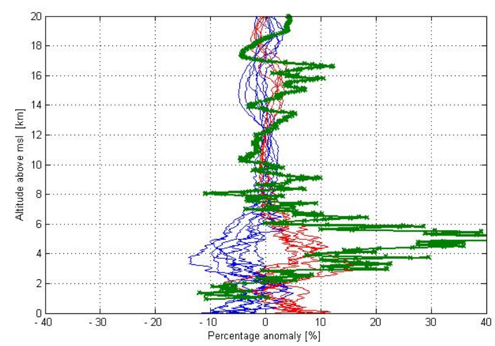

Figure 2. Bending angle percentage anomalies. Blue lines are the anomaly profiles during no TC season (Nov-May), red lines are the anomaly profiles during TC season (Jun-Oct) and the green bold line is the bending angle anomaly profile during Bertha.

In the UT, between 14 and 18 km, the bending angle anomaly increases during the TC season and this variation is generally larger during the hurricane. The RO profile was acquired from COSMIC the 8th of July 2008 at 2:01, at the time when Bertha was a major hurricane (Cat. 3) slowly moving to the north-west (less than 10 km per hour). The cyclone diameter was about 400 km, the eye diameter 30 km and the location of the RO as provided by CDAAC was 117 km from the center.

All the eight cases that we analyzed during Bertha, presented the same bending angle anomaly behaviour, i.e., a large increase in the lower troposphere (between 4 and 8 km), a decrease around 10 km, and again an increase usually between 14 and 18 km (in this case more than 10%). This variation seems to be present for a long time after the event, since the average anomaly in august has the same trend, although not as large.

Fig. 3 shows the comparison of percentage anomalies for bending angle, refractivity, temperature, pressure and water vapour mixing ratio. Refractivity anomaly behaviour is similar to bending angle anomaly but much more attenuated. This can be explained by the fact that the bending angle depends on the refractivity vertical gradients, although the relation is not straight-forward. The temperature anomaly in the upper troposphere is completely symmetric to refractivity. The water vapour mixing ratio anomaly is in agreement with the bending angle anomaly in the lower troposphere but they usually have different trend in the UT. Comparing these profiles with the co-located ECMWF profiles, it seems that the model influences the derived mixing ratio profiles in the UT/LS to a large degree. The trend of mixing ratio is always determined by the model, but the 1Dvar derived mixing ratio usually has more variation than the model and reflects most of the bending angle variations when the model anomaly is positive.

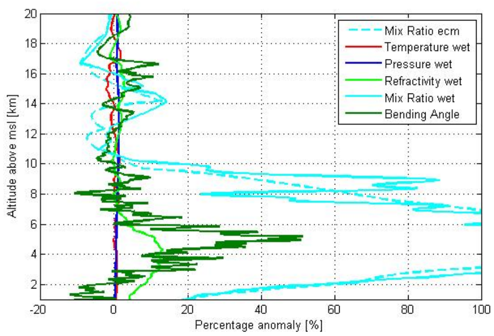

Figure 3. Comparison of percentage anomalies.

Analysing the MLS mixing ratio profile during Bertha, we see (Fig.4) an increase of mixing ratio with respect to the annual and monthly average, confirming the results of Folkins [24]. Due to the low MLS vertical resolution, it is difficult to see a direct relation between bending angle and mixing ratio here, but it is clear that there is an increase of both anomalies in the UT during the TC season. A similar trend is observed when comparing with the CALIPSO relative humidity product (not shown).

Finally, the temperature profiles show the TCs warm core and a cold peak reached in the UT/LS. As we can see from Fig. 5a, the temperature is warmer than the monthly and annual averages, up to 12 km, but above this altitude it becomes colder for a few km and then again warmer. This trend is confirmed from all the instruments we used in this work as shown in Fig. 4b and it is reasonably related with previous studies [25-28].

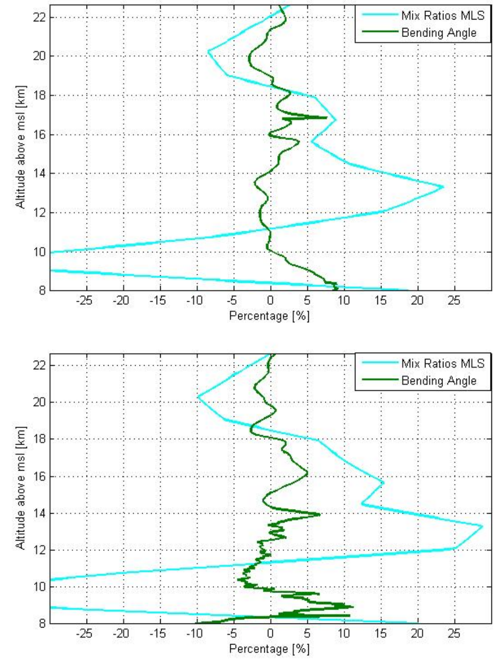

Figure 4. Green line is the bending angle anomaly, cyan line is the MLS mixing ratio anomaly. The top figure is on 8th July at 14.19 and the bottom on 10th July at 04.36.

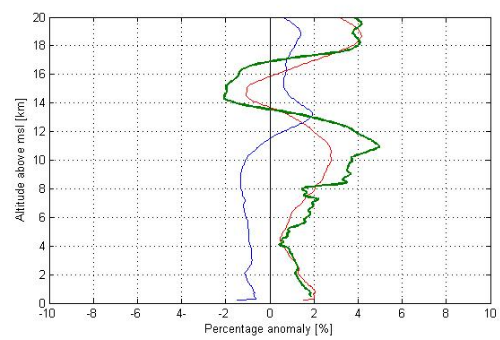

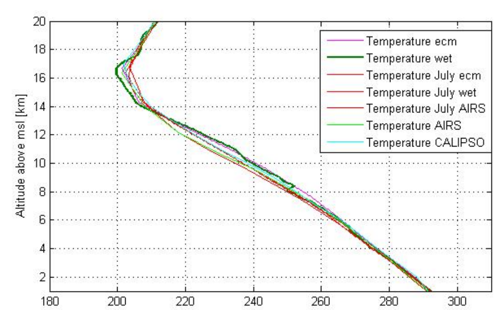

Figure 5a. Temperature anomaly profiles. Blue line is the average profile during not TC season (Nov-May), red line is the average profile during TC season (Jun-Oct) the green bold line is the temperature profile during Bertha and the light green line is the annual average.

Figure 5b. Temperature profiles comparison from different instruments.

5. DISCUSSION AND CONCLUSIONS

Our results suggest that the bending angle of a GPS radio occultation signal contains interesting information on the atmosphere around the tropopause above tropical cyclones (TC). Temperature and refractivity profiles from the COSMIC mission often show a variation at the same altitudes as the bending angle, but the signature is less pronounced and sometimes not evident. The water vapour anomalies from COSMIC agree largely with those of ECMWF, which can be explained by the fact that the ECMWF model is used in the derivation of the water vapour profiles. Thus, there could potentially be water vapour variations in the UT/LS although not present in the GPS water vapour retrievals. Comparisons with A-TRAIN instruments data show also a close agreement between RO bending angle profiles and the mixing ratio profiles. Whereas some satellite instruments are sensitive to temperature and humidity, they are often nadir-pointing with limited resolution in altitude. In this initial study we conclude that GPS ROs taken from the ISS are likely to complement such data by providing enhanced vertical resolution and thus can be useful for studies of TC convection by improving the measurement accuracy in altitude and time. Supported by simultaneous observations of cloud structure by optical cameras ROs from the ISS may then help address questions relating to overshoot of clouds across the tropopause into the lower stratosphere and the associated water vapour transport.

REFERENCES

1. Manabe S. & Wetherald, R.T. (1967). Thermal equilibrium of the atmosphere with a given distribution of relative humidity. *Journal of Atmospheric Sciences.* **24**, 241-259.

2. Forster P.M. & Shine, K.P. (1999). Stratospheric water vapour changes as a possible contributor to observed stratospheric cooling. *Geophysical Research Letters.* **26**, 3309-3312.

3. SPARC water vapour working group (2000). SPARC assessment of upper tropospheric and stratospheric water vapour. WCRP 113, WMO/TD No. 1043, SPARC report No. 2

4. Soden, B.J. & Fu, R. (1995). A satellite analisys of deep convection, upper tropospheric humidity and the greenhouse effect. *Journal of Climate,* **October 1995** (8), 2333-2351

5. Svehla, D., Rothacher, M., Ziebart, M. & Salomon, C. (2006). Galileo on board International Space Station and synergy with the ACES clock ensemble. EGU General Assembly, Vienna 2-7 April 2006

6. Neubert, T., Budtz-Jørgensen, C., Kuvvetli, I., Østgaard, N., Reglero, V. & Arnold, N., (2006). The Atmosphere-Space Interactions Monitor (ASIM) for the International Space Station. ILWS workshop, GOA, February 19-20, 2006

7. Forster, P. M. d. and Shine, K. P., Assessing the climate climate impact of trends in stratospheric water vapor. *Geophys. Res. Lett*., **29** (6):10 1 – 10 2, 2002.

8. Soden, B.J., Jackson, D.L., Ramaswamy, V., Schwarzkopf, M.D. & Huang, X. (2005). The radiative signature of upper tropospheric moistening. *Science*, **310**, 841-844, doi:10.1126/scince.1115602

9. Udelhofen, P.M. & Hartmann, D.L., (1995). Influence of tropical cloud systems on the relative humidity in the upper troposphere, *Journal of Geophysical Research,* **100**, 7423-7440

10. Khaykin, S., Pommereau, J.-P., Korshunov, L., Yushkov, V., Nielsen, J., Larsen, N., Christensen, T., Garnier, A., Lukyanov, A., and Williams, E., Hydration of the lower stratosphere by ice crystal geysers over land convective systems, *Atmos. Chem. Phys.*, **9**, 2275-2287, 2009.

11. Nielsen, J. K., Larsen, N., Cairo, F., Di Donfrancesco, G., Rosen, J. M., Durry, G., Held, G., and Pommereau, J. P.: Solid particles in the tropical lowest stratosphere, *Atmos. Chem. Phys.*, **7**, 685-695, 2007.

12. Romps, D.M. & Kuang, Z. (2009). Overshooting convection in tropical cyclones. *Geophysical Research Letters*, L09804(36).

13. Ray, E.A., & Rosenlof, K.H. (2007). Hydration of the upper troposphere by tropical cyclones. *Journal of Geophysical Research*, D12311(112).

14. Braun, J.J., Van Hove, T., & Mayo, T. (2007). Observed integrated moisture fields within tropical storm systems. 11th Symposium on Integrated Observing and Assimilation Systems for the Atmosphere, Oceans, and Land Surface (IOAS-AOLS).

15. Bath, G.S., Chakraborty, A., Nanjundiah, R.S. & Srinivasan, J. (2002). Vertical thermal structure of the atmosphere during active and weak phases of convection over north Bay of Bengal: observation and model results. *Current Science India,* **83** (3), 296-302.

16. Sherwood, S.C., Horinouchi, T. & Zeleznik, H.A. (2003). Convective impact on temperatures observed ear the tropical tropopause. *Journal of atmospheric Sciences,* **60** (15), 1847-1856.

17. Hyun Cheol Kim (2005). The effect of deep convection on temperatures in the tropical tropopause layer and its implications to the

regulation of tropical lower stratospheric humidity. PhD Thesis.

18. Kursinski, E.R., Hajj, G.A., Schofield, J.T., Linfield, R.P. & Hardy, K.R. (1997). Observing Earth's atmosphere with radio occultation measurements using the Global Positioning System. *J. Geophys. Res.*, **102**, 23429-23465.

19. Rocken C., Anthes, R., Exner, M., Hunt, D., Sokolovskiy, S., Ware, R., Gorbunov, M., Schreiner, W., Feng, D., Herman, B., Kuo, Y.H. & Zou, X. (1997). Analysis and validation of GPS/MET data in the neutral atmosphere. *J. Geophys. Res.*, **102**, 29849-29860.

20. Wickert, J., Reigber, C., Beyerle, G., Konig, R., Marquardt, C., Schmidt, T., Grunwaldt, L., Galas, R., Meehan, T.K., Melbourne, W.G. & Hocke, K. (2001). Atmosphere sounding by GPS radio occultation: First results from CHAMP. *Geophys. Res. Lett.*, **28**, 3263-3266.

21. Hajj, G.A. , Ao, C.O., Iijima, B.A., Kuang, D., Kursinski, E.R., Mannucci, A.J., Meehan, T.K., Romans, L.J., de la Torre Juarez, M. & Yunck, T.P. (2004). CHAMP and SAC-C atmospheric occultation results and intercomparisons. *J. Geophys. Res.*, **109**, D06109, doi:10.1029/2003JD003909.

22. Anthes, R.A., Bernhardt, P.A., Chenc, Y., Cucurull, L., Dymond, K.F., Ector, D., Healy, S.B., Ho, S.P., Hunt, D.C., Kuo, Y.H., Liu, H., Manning, K., McCormick, C., Meehan, T.K., Randel, W.J., Rocken, C., Schreiner, W.S., Sokolovskiy, S.V., Syndergaard, S., Thompson, D.C., Trenberth, K.E., Wee, T.K., Yen, N.L. & Zeng, Z. (2008). The COSMIC/Formosat/3 mission: Early results. *Bull. Amer. Meteor. Soc.* **89**(3), 313-333.

23. Kuo, Y.-H., Wee, T.-K., Sokolovskiy, S., Rocken, C., Schreiner, W., Hunt, D. & Anthes, R.A. (2004). Inversion and error analysis of GPS radio occultation data. *J. Meteor. Soc. Japan*, **82**, 507-531.

24. Folkins, I., & Martin, R.V. (2005). The vertical structure of tropical convection and its impact on the budgets of water vapor and ozone. *Journal of the atmospheric sciences*, **May 2005**(62), 1560-1573

25. Knaff, J.A., Zehr, R.M., Goldberg, M.D., & Kidder, S.Q. (2000). An example of temperature structure differences in tow cyclone systems derived from the Advanced Microwave Sounder Unit. *Weather and forecasting*, **August 2000**(15), 476-483.

26. Singh, D. (2008). Monitoring tropical cyclone evolution with NOAA satellites microwave observations. *Indian Journal of Radio Space Physics.* **June 2008**(37), 179-184.

27. Kidder, S.Q., Goldberg, M.D., Zehr, R.M., DeMaria, M. Purdom, J.F.W., Velden C.S., Grody, N.C., & Kusselson, S.J. (2000). Tropical cyclone analysis using AMSU data. 10th Conference on Satellite Meteorology and Oceanography.

28. Cairo, F., Buontempo, C., MacKenzie, A.R., Schiller, C., Volk, C.M., Adriani, A., Mitev, V., Matthey,R., Di Donfrancesco, G., Oulanovsky, A., Ravegnani, F., Yushkov, V., Snels, M., Cagnazzo, C., & Stefanutti,L. (2008). Morphology of the tropopause layer and lower stratosphere above a tropical cyclone: a case study on cyclone Davina (1999). *Atmospheric Chemistry and Physics*. **8**, 3411-3426.